Fluorophosphate glasses doped with Eu^{3+} and Dy^{3+} for X-ray radiography

Iago Carvalho Pinto [a,*], Gustavo Galleani [a], Luiz Gustavo Jacobsohn [b], Yannick Ledemi [c], Younes Messaddeq [c], Andrea Simone Stucchi de Camargo [a,*]

[a] São Carlos Institute of Physics, University of São Paulo, Av. Trabalhador Sãocarlense 400, 13566-590 São Carlos – SP, Brazil
[b] Department of Materials Science and Engineering, Clemson University, Clemson, SC 29634, USA
[c] Centre d'Optique, Photonique et Laser (COPL), Université Laval, 2375 rue de la terrasse, Québec, QC, Canada, G1V 0A6

ARTICLE INFO

ABSTRACT

In this work, fluorophosphate glass samples with the composition $35NaPO_3$–$30Ba(PO_3)_2$–$25MgF_2$–$(10-x)YF_3$–$x[EuF_3$ or $Dy_2O_3]$ with x = 0–4.0 mol% EuF_3, or x = 0–1.0 mol% Dy_2O_3, were fabricated by the melt quenching technique. The glasses were characterized from the structural, thermal and optical-spectroscopic points of view. Emission spectra were measured in the visible range upon UV excitation. Luminescence decay curves were registered by monitoring the most intense emissions of Eu^{3+} ($^5D_0 \rightarrow ^7F_2$) and of Dy^{3+} ($^4F_{9/2} \rightarrow ^6H_{13/2}$) in the red and green, respectively, and from them the average lifetime values of the excited states $^5D_0$ of Eu^{3+} (2.5 ms) and $^4F_{9/2}$ of Dy^{3+} (0.71 ms) were determined. Emission spectra measured under variable excitation power yielded calibration curves for Eu^{3+} and Dy^{3+}-doped glasses. The response to X-ray excitation was evaluated through radioluminescence measurements. The results indicate the promising application of these glasses in scintillators and for X-ray sensing devices.

1. Introduction

Scintillation corresponds to luminescence induced by ionizing radiation, and scintillators can be considered as wavelength shifters since emission happens at wavelengths higher than the excitation ones [1]. Scintillators are essential in applications involving the detection of ionizing radiation in the fields of medicine, security, astrophysics, oil-logging and high-energy physics [2–6]. They are usually composed of a versatile combination of a host matrix and an appropriate luminescence center [7]. Nowadays, a wide variety of materials presenting scintillation are known, e.g., organic and inorganic crystals [7,8], fluids [9], gases [10], polymers [11], and glasses [12]. Among them, inorganic crystals currently hold the biggest share of the market [13]. However, single crystals have many undesirable characteristics, such as vulnerability to moisture (e.g., NaI:Tl) and the limitations of sizes and shapes [1]. Because of that, trivalent rare earth (RE) doped glasses have been investigated as a promising alternative for crystal scintillators due to their lower cost production and easier fabrication in different sizes and shapes [6,14].

There are some important features to consider when designing a performant scintillator, such as high density, light yield, optical transparency, excited state decay times, emission spectral shape and chemical stability [1]. Among the possible host matrices, suitable for glass scintillators, phosphate glasses are attractive for their ability to bear high concentrations of rare earth ions and exhibit high optical transparency specially in the UV range [15]. However, most of them contain alkali metal ions in their composition leading to high quantity of non-bridging oxygen atoms and defects, which contributes to the increase of non-radiative energy losses and lowers the fluorescence quantum efficiency of doped glasses [16,17]. On the other hand, it is known that the addition of fluoride compounds to phosphate matrices is expected to decrease their phonon energy and decrease their hygroscopic behavior. As the fluoride content is increased, the number of hydroxyl groups (OH) in the glass network decreases. Therefore, a lower content of bridging oxygens is formed [18–20] and a fluoride-dominated environment is made available for the luminescent dopant ions, favoring their radiative emissions [21]. Hence, fluorophosphate glasses can combine characteristics of both fluoride and phosphate glasses, with the potential to host fairly large quantities of RE ions. Moreover, these glasses are usually transparent from near UV to mid infrared, and exhibit high RE quantum efficiency [22]. While scintillator glasses are commonly doped with Ce^{3+} ions [23–25], other RE activators have recently received increasing consideration. Europium ions are attractive due to their narrow and intense emission bands in the red and orange spectral regions corresponding to transitions between the excited state $^5D_0$ and the

---

* Corresponding authors.
E-mail addresses: iagocpp@gmail.com (I.C. Pinto), andreasc@ifsc.usp.br (A.S.S. de Camargo).

Table 1
Sample identification according to nominal composition.

Name	NaPO$_3$ (mol%)	Ba (PO$_3$)$_2$ (mol%)	MgF$_2$ (mol%)	YF$_3$ (mol%)	EuF$_3$ (mol%)	Dy$_2$O$_3$ (mol%)
NBYM:0.0	35	30	25	10.0	0	0
NBYM:0.10 Eu	35	30	25	9.90	0.10	0
NBYM:0.50 Eu	35	30	25	9.50	0.50	0
NBYM:1.00 Eu	35	30	25	9.00	1.00	0
NBYM:1.50 Eu	35	30	25	8.50	1.50	0
NBYM:2.00 Eu	35	30	25	8.00	2.00	0
NBYM:4.00 Eu	35	30	25	6.00	4.00	0
NBYM:0.25 Dy	35	30	25	9.75	0	0.25
NBYM:0.50 Dy	35	30	25	9.50	0	0.50
NBYM:1.00 Dy	35	30	25	9.00	0	1.00

lower energy lying $^7F_{(0-4)}$ states [20]. For example, Eu^{3+} doped glass scintillators were investigated for proton imaging [26] and neutron detection [27]. Alternatively, Dy^{3+} ions are also being considered as activators because of the intense emissions in the yellow (577 nm, $^4F_{9/2} \rightarrow {}^6H_{13/2}$ transition) and in the blue (482 nm, $^4F_{9/2} \rightarrow {}^6H_{15/2}$) spectral regions [28,29]. Further, to this date, only limited effort has been invested on the investigation of fluorophosphate glasses as scintillators, and for light detection within the UV–visible range only Ce has been used as the activator in these glasses [30–35]. For the past ten years, our research group has explored various fluorophosphate glass compositions for different optical applications and, in the present work, we report the fabrication of Eu^{3+} and Dy^{3+}-doped glasses on the compositional system NaPO$_3$-Ba(PO$_3$)$_2$-MgF$_2$-YF$_3$ and their structural and spectroscopic characterization in view of possible application as scintillators for X-ray detection.

2. Experimental

Eu^{3+} or Dy^{3+} doped glasses were prepared with the host matrix composition 35NaPO$_3$-30Ba(PO$_3$)$_2$-25MgF$_2$-(10-x)YF$_3$ with x being the molar concentration of EuF$_3$ (0.0; 0.1; 0.5; 1.0; 1.50; 2.0 and 4.0 mol%) or Dy$_2$O$_3$ (0.0; 0.25; 0.5 and 1.0 mol%). Compositions with higher concentration of barium phosphate were also considered to increase the density of the glass, but the melt crystallized during the quenching process. All the samples were prepared by the conventional melt-quenching technique. The precursor oxides and fluorides (99.99% purity) were weighted, homogeneously mixed and transferred to a capped platinum crucible (to avoid fluorine loss) before being subjected to melting in a conventional furnace. The batches were kept at 1100 °C during 1 h for homogenization of the liquid, poured into a pre-heated steel brass mold at 350 °C, and annealed at 400 °C for 3 h to eliminate internal stresses due to thermal shock. After this time the furnace was turned off and samples cooled to room temperature. Bulk samples were polished using ethyl alcohol and silicon carbide (SiC - Struers) sieves, with decreasing grain size of 800 (20–24 μm), 1200 (13–16 μm), 2400 (7–10 μm) and 4000 (< 6 μm) and finishing with 0.5 and 0.3 μm alumina suspensions, to improve optical quality. The samples were identified by their compositions, as follows: Table 1.

Table 2 presents a summary of the most relevant scintillating properties of the NBYM glasses presented in this work in comparison

to other glass scintillators for x-ray radiography reported in the literature.

The samples were characterized by X-ray diffraction (XRD) using an X-ray diffractometer model Rigaku Ultima IV in the 2θ range 10° to 70° in steps of 0.02° and a 2°/min rate. The density values were measured based on Archimedes' principle using distilled water at room temperature (ρ = 0.9976 g.cm^{-3}) in a home-made apparatus. Molar volumes were calculated based on density and molecular weight of the samples.

Thermal analysis, differential scanning calorimetry (DSC) was performed using a differential scanning calorimeter model DSC 404 from Netzsch, in the range from 50 to 750 ºC under nitrogen atmosphere at a flow rate of 20 mLmin^{-1} and a heating rate of 10 °C/min. Thermal analysis was done to determine the characteristics temperatures of the glasses, i.e. the glass transition and the onset of crystallization, Tx. Raman scattering measurements were performed at room temperature using a LabRam HR spectrometer from Horiba-Jobin Yvon with a 1200 grooves/cm grating. The 632 nm line from an argon ion laser was focused on the bulk samples by an optical microscope using a long work distance 50X objective.

Optical absorption spectra were recorded using a Perkin Elmer spectrophotometer model Lambda 1050 in the 350–750 nm range for 2 mm thick samples. Photoluminescence spectra were measured at room temperature in a Horiba Jobin Yvon spectrofluorimeter model Fluorog FL-1050, equipped with a CW Xe lamp as the excitation source. The signals were collected by a photodiode detector (model PPD-850) from 250 nm to 700 nm. The luminescence decay curves of Eu^{3+} and Dy^{3+} were measured using the same equipment with detection by a PMT detector. The average excited state lifetime values (τ_1) of $^5D_0$ (for Eu^{3+}) and $^4F_{9/2}$ (for Dy^{3+}) were determined by fitting the curves with single exponential functions. Excitation power dependent emission spectra were measured in the 3.5–25 mW range, as determined by a laser power meter, using a 360 nm solid-state laser from Laser Glow Technologies, in a Horiba Jobin Yvon spectrofluorimeter model Fluorog FL-1050.

Radioluminescence (RL) measurements were carried out using a customer-designed Freiberg Instruments Lexsyg Research spectrofluorometer equipped with a Varian Medical Systems VF-50 J X-ray tube with a tungsten target. The X-ray source was coupled with an ionization chamber for continuous irradiation monitoring. The light emitted by the sample was collected by a lens and converged into an optical fiber connected to an Andor Technology Shamrock 163 spectrograph coupled to a cooled (−80 °C) Andor Technology DU920P-BU Newton CCD camera. RL measurements were executed under continuous X-ray irradiation (40 kV, 1 mA) at room temperature. Glass powders filled ca. 8 mm diameter 0.5 mm deep cups thus allowing for relative RL intensity comparison between different samples.

3. Results and discussion

3.1. Sample preparation and structural characterization

The choice of a fluorophosphate glass composition to study the scintillating properties of Er^{3+} and Dy^{3+} was based on the fact that reports of scintillation of fluorophosphate glasses doped with RE

Table 2
Scintillating properties of NBYM glasses and other glass scintillators for x-ray radiography reported in literature.

Scintillator	Density (g/cm^3)	Most intense emission (nm)	Luminescent lifetime (ms)
NBYM:4.0 Eu	3.65	611	≈2.5
NBYM:0.25 Dy	3.66	572	≈0.78
Dy^{3+}-activated Lithium-borate glasses [58]	2.72	572	≈0.44
Eu^{3+}-doped gadolinium calcium fluorophosphate [18]	3.15	611	≈2.24
IQI301 (Tb^{3+}-doped silicate glass) [37]	3.80	550	≈3.0
Tb^{3+}-doped phosphate glasses [64]	4.01	544	≈1.66

ions are quite rare in the literature. The combined characteristics of fluoride and phosphate glass like good thermal stability and rather low phonon environment that improves RE emission intensities are promising for this purpose. The choice of the dopant ions Eu^{3+} and Dy^{3+} as activators was based on their narrow and intense emissions in the red and yellow spectral region, that can be particularly interesting for scintillators aimed at X-ray detection. The prepared samples were essentially colorless and exhibit high optical transparency to the naked eye. The amorphous nature of the glass was revealed by XRD measurements (not shown).

As widely known, the density of the glasses slightly increase with the increase of the dopant concentration since the incorporation of the heavier EuF_3 was accomplished by direct substitution of YF_3 without any additional changes in the composition of the glasses. Since molar volume is inversely proportional to the density, it decreased with increasing dopant concentration. Higher glass density increases the probability of absorption of incoming X-rays, hence enhancing the efficiency of the glass scintillator [62,63]. The samples presented superior density values when compared with commercially available Ce^{3+} activated lithium borate glass scintillators (~2.50 g/cm^3) [38,39], and similar density values when compared with the inorganic single crystal scintillator NaI:Tl (3.67 g/cm^3) [36] and commercially available glass scintillators for X-ray radiography (3.8 g/cm^3) [37]. The ionic densities of the Eu^{3+}-doped samples for 0.5%, 1.0%, 2.0% and 4.0% mol are 0.69, 1.40, 2.81 and 5.61 × 10^{20} $ions/cm^3$, respectively. These values are slightly higher than those reported for other Eu^{3+}-doped fluorophosphate glasses in the literature [49,51]. For Dy^{3+}-doped samples the ionic densities for 0.25%, 0.5% and 1.0% mol were found to be 0.66, 1.36 and 2.81 × 10^{20} $ions/cm^3$, respectively. These results are similar to those reported for other fluorophosphate glasses [59], and higher than those reported for lead borate glasses [56].

Thermal characterizations performed in the glass matrix (NBYM:0,0) revealed a glass transition temperature T_g = 480 °C, and the crystallization temperature T_c = 653 °C. These results yield the thermal stability parameter T_c - T_g = 173 °C. The thermal properties are similar to those obtained for other fluorophosphate [40,42] and phosphate glasses [41]. The addition of Eu^{3+} and Dy^{3+} had no significant influence on the thermal properties of the glasses.

A representative Raman spectrum of the glass matrix (NBYM:0,0) is shown in Fig. 1, and similar results were found for the doped samples. Six characteristic bands were observed at 341, 489, 737, 952, 1045 and 1111 cm^{-1}. The 341 cm^{-1} band indicates the presence of alkali-oxides such as Na_2O [43]. The band at 489 cm^{-1} is related to the symmetric stretching vibrations of Mg-F bonds [44], while that
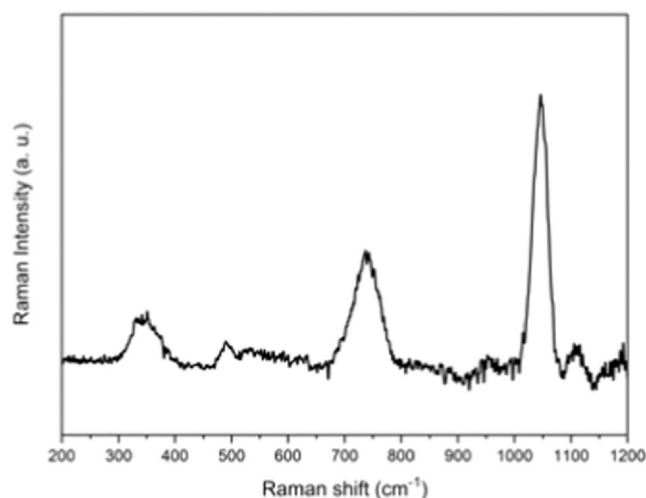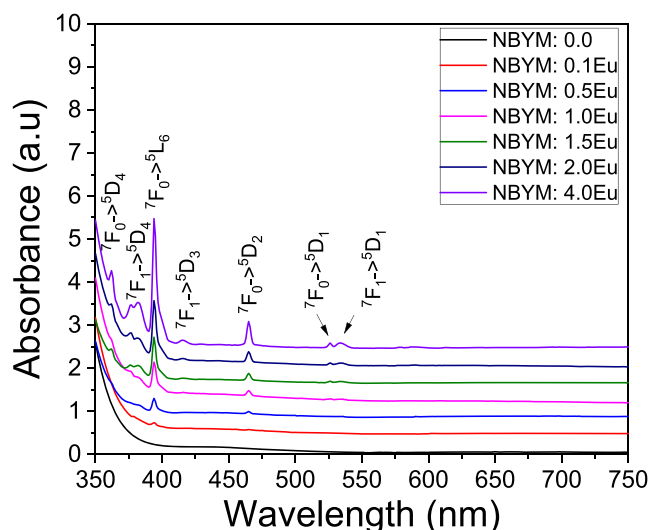

Fig. 2. Absorption spectra of Eu^{3+} doped glasses. Spectra are vertically shifted to enhance visual clarity.

at 737 cm^{-1} is related to the P-O-P symmetric stretching mode [45]. The bands at 952, 1045 and 1111 cm^{-1} are related to stretching vibrations of non-bridging oxygens in diverse PO_4 environments: $Q^{(0)}$ (orthophosphate), $Q^{(1)}$ (pyrophosphate), $Q^{(2)}$ (metaphosphate), respectively [42–44]. The maximum phonon energy ($h\omega$) of the glass is found around 1110 cm^{-1}, corresponding to the vibrational band with highest intensity [43]. These results are similar to those reported for similar structures of fluorophosphate- [43–46] and phosphate [47] glasses.

3.2. Photophysical characterization of Eu^{3+}-doped glasses

The absorption spectra of Eu^{3+} doped samples are presented in Fig. 2 with a vertical offset of 0.4 a.u. in the intensity axis for better visualization. Besides the intense absorption around 390 nm, the spectra show six other transitions originating from the ground states $^7F_0$ and $^7F_1$, as indicated in the figure. The glass matrix presents good transparency in the visible spectral range as very low absorption coefficients are observed between 400 and 750 nm. These results are similar to those presented by Binnemans [48], who reported on the spectroscopic characteristics of Eu^{3+} in different hosts.

The photoluminescence excitation spectra of the Eu^{3+}-doped glasses (Fig. 3(a)) were measured in the range 310–500 nm, monitoring the emission corresponding to the most intense transition at 611 nm ($^5D_0 \rightarrow {}^7F_2$). As it can be seen, the most intense excitation peak is at 393 nm, in accordance with the absorption spectra in Fig. 2. Therefore, this wavelength was chosen to excite the emission spectra that are presented in Fig. 3(b) in the 500–750 nm range.

Photoluminescence decay curves corresponding to the red emission ($^5D_0 \rightarrow {}^7F_2$ transition at 611 nm) were fit by single exponential decay functions (see Fig. 4) and yielded the average lifetime value τ_1 = 2.5 ms for all Eu-doped samples. This favorable result indicates no evidence of non-radiative energy transfer activation between Eu^{3+} ions (which would imply decreased τ values), as the concentration increases from 0.1 to 4.0 mol%. Thus, provided that no clustering formation takes place, there is a perspective that the glasses might be able to host higher doping concentrations leading to higher absorption coefficient and improved UV–visible conversion efficiency. The lifetime results are in accordance with the values found for Eu^{3+} doped fluorophosphates glasses studied by Sreedhar et al. [49] and Shoaib et al. [51–53], and are similar to those of commercially available glasses for X-ray radiography (~3 ms) [37].

Fig. 1. Raman shift representative spectrum of the NBYM:0,0 glass.
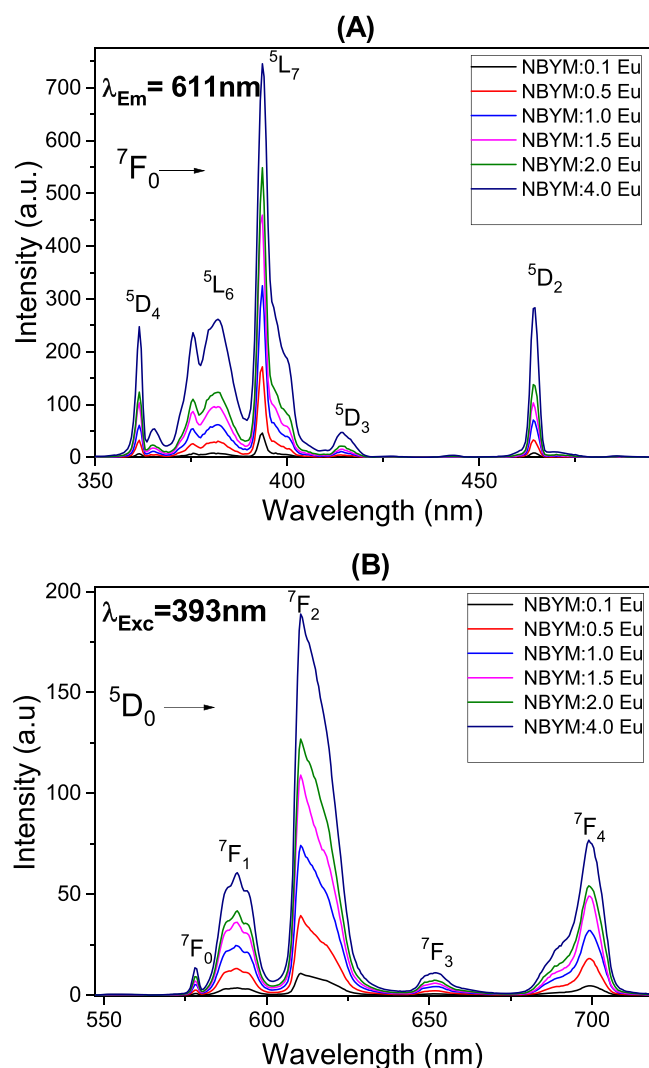
Fig. 3. Photoluminescence excitation (A) and emission (B) spectra of the Eu^{3+}-doped samples.
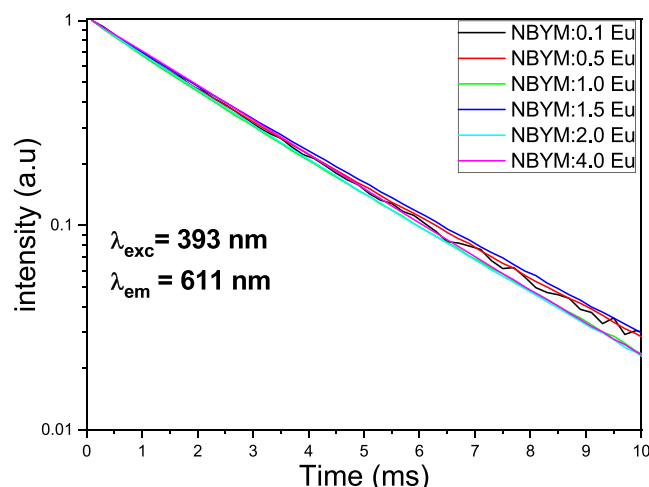

Fig. 4. Luminescent decay curves for Eu^{3+} doped glasses.

The emission spectra measured with varying excitation power at 360 nm are presented in Fig. 5. The shape of the characteristic bands barely changes with the increasing excitation power. Furthermore, photoluminescence intensity as determined by the area below the
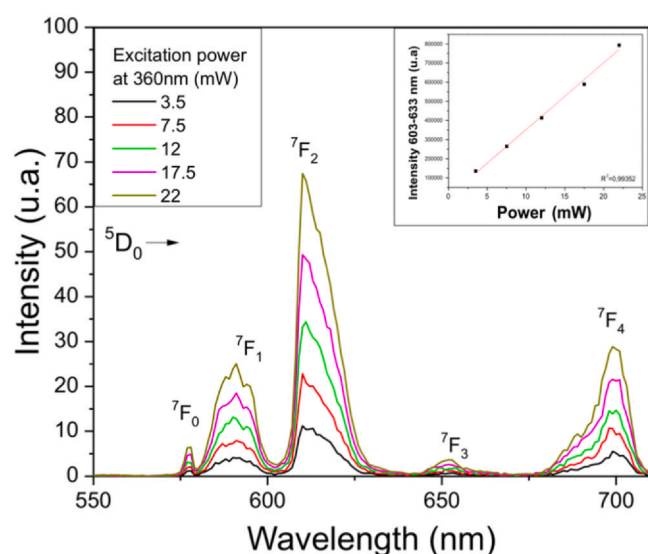

Fig. 5. Emission spectra of Eu^{3+}-doped fluorophosphate glasses as a function of excitation power ($\lambda_{exc} = 360$ nm). The inset shows the linear relation between the area below bands in the 603–633 nm range and the laser power.
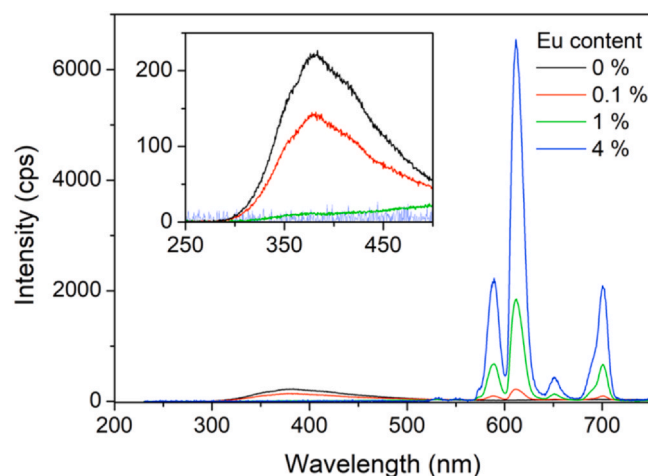

Fig. 6. Radioluminescence spectra of Eu^{3+}-doped glasses, where the inset highlights the host defect band centered at 380 nm.

bands within the 603–633 nm range increases proportionally with increasing power up to 22 mW, as shown in the inset in Fig. 5.

Fig. 6 shows the results of radioluminescence measurements under X-ray excitation. The spectra show increasing emission intensity with the increasing concentration of Eu^{3+}, corroborating the excited state lifetime results that indicate no sign of concentration quenching. Furthermore, the spectra reveal a broad emission band around 380 nm for the undoped and lowly doped (0.1 mol%) glass, which is attributed to host defects. A similar broad band ranging from 380 to 450 nm was detected in X-ray irradiated fluorophosphate glass reported in the literature [60]. The intrinsic X-ray induced defect centres are mainly caused by holes trapped on phosphate groups - the so-called phosphorus-oxygen hole centres (POHC). It has been shown that the absorption due to intrinsic POHC is removed when doped with Eu^{3+} [60,61]. The intensity of this band decreases with increasing Eu content, being reduced by about 30% already with the incorporation of only 0.1 mol% of Eu^{3+} (cf. inset in Fig. 6). This is in agreement with absorption results shown in Fig. 3(a) where Eu^{3+} presents broad absorption band around 380 nm corresponding to the $^7F_0 \rightarrow {}^5L_7$ transition that overlaps with the defect emission.
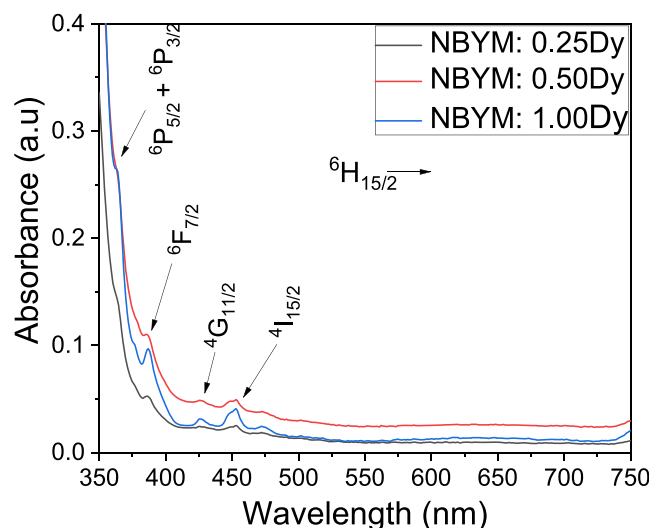
Fig. 7. Absorption spectra of Dy³⁺ doped fluorophosphates glass samples.

3.3. Photophysical characterization of Dy³⁺-doped glasses

Absorption spectra of Dy³⁺ doped glasses can be seen in Fig. 7. The characteristic Dy³⁺ absorption bands are observed at 349, 363, 425 and 450 nm, which are related to transitions from the ground state $^6H_{15/2}$ to $^6P_{5/2}$ +$^6P_{3/2}$, $^6F_{7/2}$, $^4G_{11/2}$ and $^4I_{15/2}$ respectively. These results are in agreement with the absorption spectra of other Dy³⁺ doped glasses as reported in [54].

The excitation photoluminescence spectra were obtained by monitoring the emission at 575 nm ($^4F_{9/2} \rightarrow {}^6H_{13/2}$ transition) in the 300–500 nm range and shown in Fig. 8(a). There are three intense excitation bands in the range 340–420 nm, and the transition $^6H_{15/2} \rightarrow {}^7P_{7/2}$ at 350 nm was used to excite the emission spectra recorded in the 450–750 nm range (Fig. 8(b)).

The emission spectra exhibit three major electronic transitions characteristic of Dy³⁺, with the most intense one corresponding to the $^5F_{9/2} \rightarrow {}^5H_{13/2}$ transition. These results are in accordance with studies made on other Dy³⁺-doped fluorophosphate and borate glasses [54–57].

Similarly, to the procedure described for Eu³⁺-doped glasses, the excited state average lifetime values were determined by fitting the luminescence decay curves corresponding to the emission at 575 nm ($^4F_{9/2} \rightarrow {}^6H_{13/2}$) with single exponential decay functions. The results ranged from 0.74 ms for the sample doped with 0.25 mol% Dy₂O₃ to 0.67 ms for the glasses with 0.5 and 1.0 mol%. Although the difference in value is not so large (~10%) it suggests that Dy³⁺ ions are more likely to suffer concentration quenching than Eu³⁺ in this glass matrix. As also shown by Anil Kumar et al. [54] the decrease in lifetime value is associated to concentration quenching, that is, non radiative energy transfer between Dy³⁺ ions followed by loss to the host matrix as the average distance between Dy³⁺ ions decreases with the increasing content of dopant [54,55]. This observation was also made by Pisarska [56] for samples of lead borate glasses doped with Dy³⁺ concentrations higher than 0.25%. Another advantage of the glass system investigated in this work is that its fluorescence lifetimes are about 4x faster than those reported from glasses used for X-ray radiography [37]. Fig. 9.

The photoluminescence emission of Dy³⁺-doped glasses was also investigated under varied excitation power (Fig. 10), which revealed a linear trend of the area of the most intense emission band at around 478 nm with increasing excitation power up to 25 mW (inset in Fig. 10).

The ability of the samples to detect X-rays was evaluated through radioluminescence measurements and the spectra are shown in
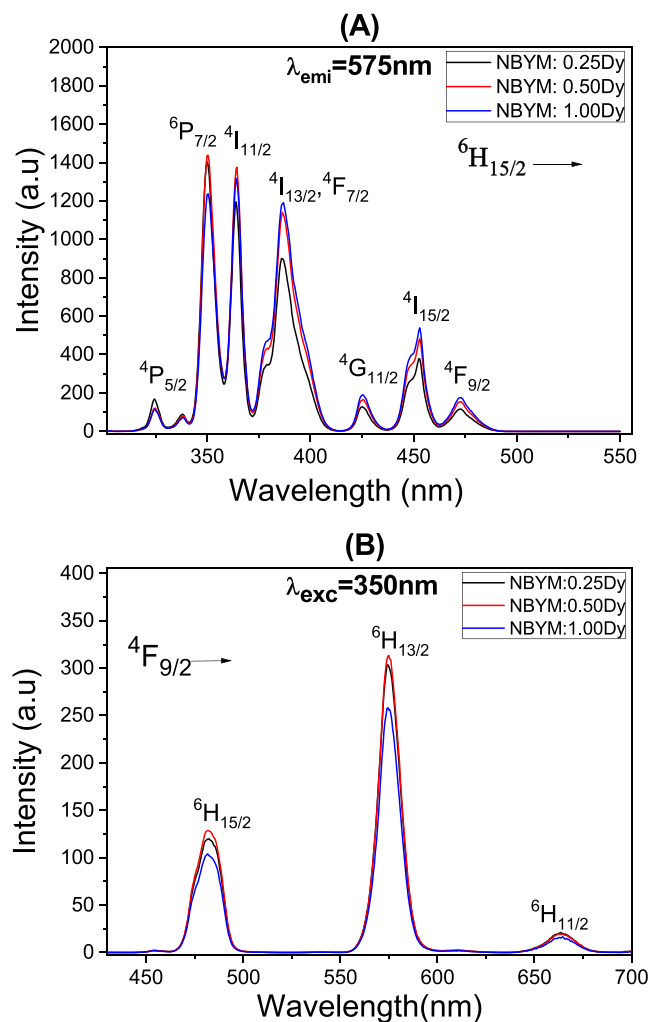

Fig. 8. (a) Photoluminescence excitation spectra (λem = 611 nm) and (b) Photoluminescence emission spectra with excitation at 350 nm of the Dy³⁺ doped fluorophosphates glasses.
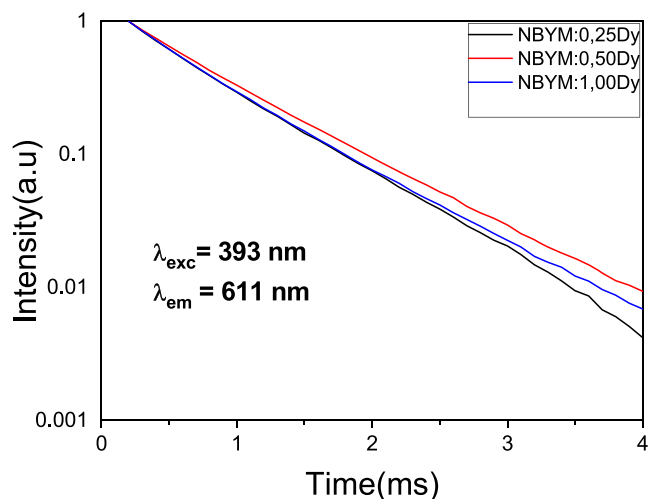

Fig. 9. Luminescent decay curves for Eu³⁺ doped glasses.

Fig. 11. The most intense emission was obtained from the glass with highest Dy concentration (1 mol%) being 13% higher than the intensity from the sample doped with 0.25 mol%. The results are in accordance with a report from Kaewnuam et al. [58] who
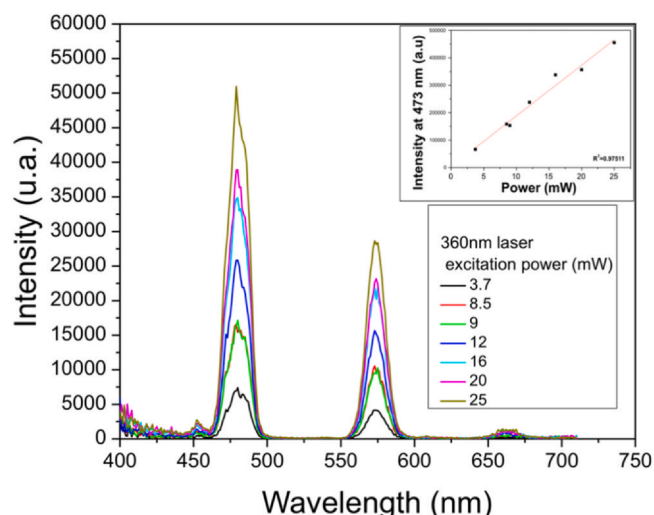
Fig. 10. Excitation power dependence of emission spectra of Dy^{3+}-doped glasses. Inset shows the calibration curve relating the emission intensity at 478 nm to the increasing power.
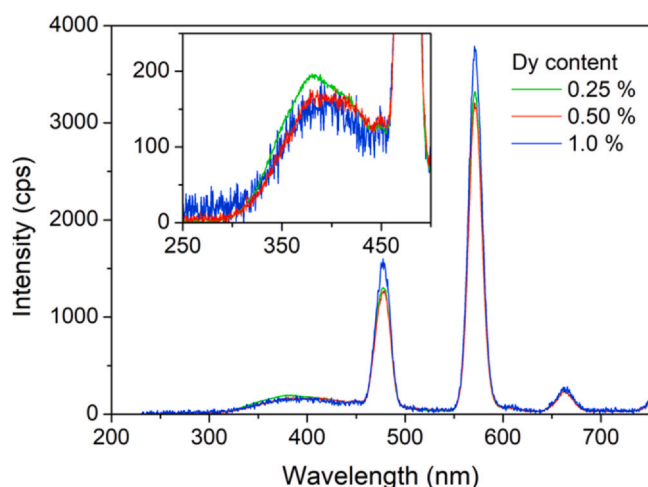

Fig. 11. Radioluminescence spectra of Dy^{3+}-doped glasses. The inset highlights the band centered at 380 nm.

investigated lithium borate glasses doped with Dy^{3+} for scintillating applications and recorded luminescent quenching with Dy^{3+} concentrations higher than 0.4 mol% under X-ray induced luminescence. The fact that this glass strongly emits at two different wavelengths, 478 and 572 nm, facilitates maximizing spectral coupling of the emission with the detection efficiency of a wide range of photodetectors. As for the defect band identified in the undoped and Eu^{3+}-doped samples around 380 nm, it is also present in the spectra of Dy^{3+}-doped samples. However, its intensity decreases only slightly with increasing Dy^{3+} concentration. This can be explained by the lower overlap between defect emission and the excitation spectrum of the Dy^{3+}-doped samples at the same spectral interval (see Fig. 8(a)) when compared to Eu^{3+} doped ones (see Fig. 3(a)).

4. Summary and conclusions

This work shows that fluorophosphate glasses doped with Eu^{3+} or Dy^{3+} ions are promising glass scintillators for X-ray detection. The glasses were reproducibly fabricated by the melt-quenching technique, and presented excellent optical properties. The samples presented superior density values when compared with commercially

available Ce^{3+} activated lithium borate glass scintillators and similar density to previously studied glass scintillators for X-ray radiography.

Glasses were able to emit on the visible spectral range (450–700 nm) when excited with ultraviolet and X-rays. In either glass, no sign of photoluminescence or radioluminescence intensity saturation was observed for the highest RE activator concentration suggesting that higher RE activator concentrations could lead to still higher luminous output. For comparison, the radioluminescence peak intensity of 4 mol% Eu^{3+} at 612 nm was 4.3x the peak intensity of 1 mol% Dy^{3+} at 478 nm and 1.7x at 572 nm. Furthermore, photoluminescence spectra were measured under varying excitation powers at 365 nm, which lead to calibration curves, for both type of doped glasses, that can be used to quantitatively detect the UV radiation. In terms of excited state lifetime values, no significant variations were observed with the increase in Eu^{3+} concentration in Eu^{3+}-doped glasses. On the other hand, Dy^{3+}-doped samples showed to be prone to concentration quenching for Dy^{3+} doping concentrations higher than 0.25 mol%. From the viewpoint of X-ray radiography, lifetimes found in this work were similar or faster to current commercially available scintillator glasses.

CRediT authorship contribution statement

A. S. S. de Camargo: was the main supervisor and provider of infrastructure of this work. She advised the Master's Dissertation of I. Carvalho Pinto, from which this work derives. **I. Carvalho Pinto:** The first author, was responsible for making the glasses, collecting all the data on characterization and writing the manuscript with the supervision of the postdoctoral researcher G. Galleani. **G. Galleani:** Participated as an informal but active co-advisor of I. Carvalho Pinto. He also took part in the writing of the manuscript. **L. G. Jacobsohn;** Performed the radioluminescence measurements at the Clemson University, South Carolina, USA, and participated in the discussions. **Y. Ledemic:** Performed the photoluminescence measurements as a function of excitation power at the University of Laval, Canada, and participated in the discussions. **Y. Messaddeq:** Provided the infrastructure at the University of Laval, Canada, and participated in the discussions.

Declaration of Competing Interest

The authors declare that they have no known competing financial interests or personal relationships that could have appeared to influence the work reported in this paper.

References

[1] C. Lecoq, Paul Annenkov, Alexander Gektin, Alexander Korzhik, Mikhail Pedrini, Inorganic Scintillators for Detector Systems, second ed.,, Springer, Berlin, Heidelberg, 2006.

[2] T. Yanagida, A. Yoshikawa, Y. Yokota, K. Kamada, Y. Usuki, S. Yamamoto, M. Miyake, M. Baba, K. Kumagai, K. Sasaki, M. Ito, N. Abe, Y. Fujimoto, S. Maeo, Y. Furuya, H. Tanaka, A. Fukabori, T.R. dos Santos, M. Takeda, N. Ohuchi, Development of Pr:LuAG scintillator array and assembly for positron emission mammography, IEEE Trans. Nucl. Sci. 57 (2010) 1492–1495.

[3] D. Mannes, F. Schmid, J. Frey, K. Schmidt-Ott, E. Lehmann, Combined neutron and X-ray imaging for non-invasive investigations of cultural heritage objects, Phys. Procedia 69 (2015) 653–660.

[4] K. Yamaoka, M. Ohno, Y. Terada, S. Hong, J. Kotoku, Y. Okada, A. Tsutsui, Y. Endo, K. Abe, Y. Fukazawa, S. Hirakuri, T. Hiruta, K. Itoh, T. Itoh, T. Kamae, M. Kawaharada, N. Kawano, K. Kawashima, T. Kishishita, T. Kitaguchi, M. Kokubun, G.M. Madejski, K. Makishima, T. Mitani, R. Miyawaki, T. Murakami, M.M. Murashima, K. Nakazawa, H. Niko, M. Nomachi, K. Oonuki, G. Sato, M. Suzuki, H. Takahashi, I. Takahashi, T. Takahashi, S. Takeda, K. Tamura, T. Tanaka, M. Tashiro, S. Watanabe, T. Yanagida, D. Yonetoku, Development of the HXD-II wide-band all-sky monitor onboard Astro-E2, IEEE Trans. Nucl. Sci. 52 (2005) 2765–2772.

[5] T. Yanagida, Y. Fujimoto, S. Kurosawa, K. Kamada, H. Takahashi, Y. Fukazawa, M. Nikl, V. Chani, Temperature dependence of scintillation properties of bright oxide scintillators for well-logging, Jpn. J. Appl. Phys. 52 (2013) 076401.

[6] S. Huang, Q. Gao, M. Gu, Enhanced luminescence in transparent glass ceramics containing BaYF5: Ce3+ nanocrystals, J. Lumin. 132 (2012) 750–754.

[7] J.Y. Lee, G. Adhikari, C. Ha, H.J. Kim, N.Y. Kim, S.K. Kim, Y.D. Kim, H.S. Lee, A study of NaI(Tl) crystal encapsulation using organic scintillators for the dark matter search, Nucl. Instrum. Methods Phys.Res. Sect. A Accel. Spectrom. Detect. Assoc. Equip. 953 (2020) 163141.

[8] T. Ogawa, D. Nakauchi, M. Koshimizu, N. Kawaguchi, T. Yanagida, Characterizations of Pr:Ca2Al2SiO7 single crystal scintillator for α-ray detection, Opt. Mater. 100 (2020) 109565.

[9] P.R. Bell, The use of anthracene as a scintillation counter, Phys. Rev. 73 (1948) 1405–1406.

[10] G.L. Braglia, G.M. de'Munari, G. Mambriani, Remarks on noble gas scintillation in an electric field, Il Nuovo Cimento B Ser. 10 43 (1966) 130–149.

[11] M. Hamel, R. Pjatkan, H. Burešová, From the R&D to the commercialization of a new green-emitting plastic scintillator, Nucl. Instrume. Methods Phys. Res. Sect. A Accel. Spectrom. Detect. Assoc. Equip. 955 (2020) 163294.

[12] Y. Zou, W. Zhang, C. Li, Y. Liu, H. Luo, Construction and test of a single sphere neutron spectrometer based on pairs of 6Li-and 7Li-glass scintillators, Radiat. Meas. 127 (2019) 106148.

[13] I. Group, Scintillator Market: Global Industry Trends, Share, Size, Growth, Opportunity and Forecast 2019–2024, (2019).

[14] T. Yanagida, Study of rare-earth-doped scintillators, Opt. Mater. 35 (2013) 1987–1992.

[15] V. V. Nagarkar, V. Gaysinskiy, Z. Bell, M. Bliss, S. Miller, K.J. Riley, A Neutron Imaging Detector from Bundled Lithium Silicate Glass Fibers, in: 2009 IEEE Nucl. Sci. Symp. Conf. Rec., 2009: pp. 1122–1125.

[16] Y. Yao, L. Liu, Y. Zhang, D. Chen, Y. Fang, G. Zhao, Optical properties of Ce3+ doped fluorophosphates scintillation glasses, Opt. Mater. 51 (2016) 94–97.

[17] A. Vedda, M. Martini, M. Nikl, E. Mihokova, K. Nitsch, N. Solovieva, F. Karagulian, Optical absorption and thermoluminescence of Tb3 -doped phosphate scintillating glasses, J. Phys. Condens. Matter 14 (2002) 7417–7426.

[18] P. Meejitpaisan, C. Kedkaew, Spectroscopic properties of Eu 3+ -doped gadolinium calcium phosphate and fluorophosphates glasses, Mater. Today Proc. 5 (2018) 13926–13933.

[19] R. Vijaya, V. Venkatramu, P. Babu, C.K. Jayasankar, U.R. Rodríguez-Mendoza, V. Lavín, Spectroscopic properties of Sm3+ ions in phosphate and fluorophosphate glasses, J. Non Cryst. Solids 365 (2013) 85–92.

[20] R. Balakrishnaiah, R. Vijaya, P. Babu, C.K. Jayasankar, M.L.P. Reddy, Characterization of Eu3+-doped fluorophosphate glasses for red emission, J. Non Cryst. Solids 353 (2007) 1397–1401.

[21] G. Galleani, S. Santagneli, Y. Messaddeq, M. De oliveira Junior, H. Eckert, Rare-earth doped fluoride phosphate glasses: structural foundations of their luminescence properties, Phys. Chem. Chem. Phys. 19 (2017) 21612–21624.

[22] V.B. Sreedhar, K. Venkata Krishnaiah, S.K. Nayab Rasool, V. Venkatramu, C.K. Jayasankar, Raman and photoluminescence studies of europium doped zinc-fluorophosphate glasses for photonic applications, J. Non Cryst. Solids 505 (2019) 115–121.

[23] L. Pan, J.K.M.F. Daguano, N.M. Trindade, M. Cerruti, E.D. Zanotto, L.G. Jacobsohn, Scintillation, luminescence and optical properties of Ce-Doped borosilicate glasses, Opt. Mater. 104 (2020) 109847.

[24] M.W. Kielty, L. Pan, M.A. Dettmann, V. Herrig, U. Akgun, L.G. Jacobsohn, J. Mater. Sci. Mater. Electron. 30 (2019) 16774–16780.

[25] M.W. Kielty, M. Dettmann, V. Herrig, M.G. Chapman, M.R. Marchewka, A.A. Trofimov, U. Akgun, L.G. Jacobsohn, Investigation of Ce3+ luminescence in borate-rich borosilicate glasses, J. Non Cryst. Solids 471 (2017) 357–361.

[26] I.J. Tillman, M.A. Dettmann, V. Herrig, Z.L. Thune, A.J. Zieser, S.F. Michalek, M.O. Been, M.M. Martinez-Szewczyk, H.J. Koster, C.J. Wilkinson, M.W. Kielty, L.G. Jacobsohn, U. Akgun, High-density scintillating glasses for a proton imaging detector, Opt. Mater. 68 (2017) 58–62.

[27] G.L. Ademoski, S. Simko, M. Teeple, I. Morrow, P. Kralik, C.J. Wilkinson, G. Varney, M. Martinez-Szewczyk, L. Yinong, J.K. Nimmagadda, S. Samant, Y. Wu, L. Pan, L.G. Jacobsohn, Q. Wilkinson, F. Duru, U. Akgun, A glass neutron detector with machine learning capabilities, J. Inst. 14 (2019) P06013.

[28] J. Kaewkhao, N. Wantana, S. Kaewjaeng, S. Kothan, H.J. Kim, Luminescence characteristics of Dy3+ doped Gd2O3-CaO-SiO2-B2O3 scintilling glasses, J. Rare Earths 34 (2016) 583–589.

[29] L. Yuliantini, E. Kaewnuam, R. Hidayat, M. Djamal, K. Boonin, P. Yasaka, C. Wongdeeying, N. Kiwsakunkran, J. Kaewkhao, Yellow and blue emission from BaO-(ZnO/ZnF2) B2O3TeO2 glasses doped with Dy3+ for laser medium and scintillation material applications, Opt. Mater. 85 (2018) 382–390.

[30] C. Jiang, J. Zhang, F. Gan, Scintillating luminescence of cerium-doped dense oxide glass, Proc. SPIE 3768, Hard X-Ray, Gamma-Ray, and Neutron Detector Physics 3768 Proc.SPIE, 1999, pp. 462–469.

[31] J. Jiang, G. Zhang, M. Poulain, Cerium-containing glasses for fast scintillators, J. Alloy. Compd. 275–277 (1998) 733–737.

[32] C. Hu, A. Margaryan, A. Margaryan, F. Yang, L. Zhang, R. Zhu, Alkali-free Ce-doped and co-doped fluorophosphate glasses for future HEP experiments, Nucl. Instrum. Methods Phys. Res. Sect. A Accel. Spectrom. Detect. Associated Equip. 954 (2020) 161665.

[33] M. Akatsuka, K. Shinozaki, D. Nakauchi, T. Kato, G. Okada, N. Kawaguchi, T. Yanagida, Scintillator and dosimeter properties of Ce3+ doped CaF2AlF3AlPO4 glasses, Opt. Mater. 94 (2019) 86–91.

[34] Y. Minami, J. Lynn, V.C. Agulto, Y. Lai, M. John, F. Empizo, T. Shimizu, K. Yamanoi, N. Sarukura, A. Yoshikawa, T. Murata, M. Guzik, Y. Guyot, G. Boulon, J.A. Harrison, M. Cadatal-raduban, Spectroscopic investigation of praseodymium and cerium co-doped 20Al(PO3)3-80LiF glass for potential scintillator applications, J. Non Crystal. Solids 521 (2019) 119495.

[35] T. Murata, Y. Arikawa, K. Watanabe, K. Yamanoi, M. Cadatal-Raduban, T. Nagai, M. Kouno, K. Sakai, T. Nakazato, T. Shimizu, N. Sarukura, M. Nakai, T. Norimatsu, H. Nishimura, H. Azechi, A. Yoshikawa, S. Fujino, H. Yoshida, N. Izumi, N. Sato, H. Kan, Fast-Response and Low-Afterglow Cerium-Doped Lithium 6 Fluoro-Oxide Glass Scintillator for Laser Fusion-Originated Down-Scattered Neutron Detection, IEEE Trans. Nucl. Sci. 59 (2012) 2256–2259, https://doi.org/10.1109/TNS.2012.2212458.

[36] G. Knoll, Radiation Detection and Measurement, John Wiley and Sons, Inc., New York, 1979, p. 831.

[37] H.E. Martz Jr., C.M. Logan, D.J. Schneberk, P.J. Shull, X-Ray Imaging, CRC Press, Boca Raton, 2017, p. 194.

[38] S. Gobain, Lithium Glass Scintillators, (n.d.).

[39] Scintacor, 6-lithium glass bespoke to your application, (n.d.).

[40] H. Sun, L. Zhang, S. Xu, S. Dai, J. Zhang, L. Hu, Z. Jiang, Structure and thermal stability of novel fluorophosphate glasses, J. Alloy. Compd. 391 (2005) 151–155.

[41] G. Tricot, B. Revel, S. Wegner, Thermal stability of a low Tg phosphate glass investigated by DSC, XRD and solid state NMR, J. Non Cryst. Solids 357 (2011) 2708–2712.

[42] R.P.R.D. Nardi, C.E. Braz, C. Pereira, C.D. Freschi, J.L. Ferrari, A.S.S. de Camargo, H. Eckert, F.C. Cassanjes, G. Poirier, Crystallization in lead tungsten fluorophosphate glasses, Mat. Res. 18 (2015) 228–232.

[43] R. Nayab, L. Moorthy, C. Jayasankar, Optical and luminescence properties of Eu < SUP > 3+ < /SUP > -doped phosphate based glasses, Mat. Express 3 (2013) 231–240.

[44] G.L. Agawane, K. Linganna, J.-H. In, J.H. Choi, High emission cross-section Er3+-doped fluorophosphate glasses for active device application, Optik 198 (2019) 163228.

[45] V.B. Sreedhar, K. Venkata Krishnaiah, S.K. Nayab Rasool, V. Venkatramu, C.K. Jayasankar, Raman and photoluminescence studies of europium doped zinc-fluorophosphate glasses for photonic applications, J. Non Crystal. Solids 505 (2019) 115–121.

[46] P. Mpourazanis, G. Stogiannidis, S. Tsigoias, A.G. Kalampounias, Transverse phonons and intermediate-range order in Sr-Mg fluorophosphate glasses, Spectrochim. Acta Part A Mol. Biomol. Spectrosc. 212 (2019) 363–370.

[47] R.J. Kirkpatrick, R.K. Brow, Nuclear magnetic resonance investigation of the structures of phosphate and phosphate-containing glasses: a review, Solid State Nucl. Magn. Reson. 5 (1995) 9–21.

[48] K. Binnemans, Interpretation of europium(III) spectra, Coord. Chem. Rev. 295 (2015) 1–45.

[49] V.B. Sreedhar, K. Venkata Krishnaiah, S.K. Nayab Rasool, V. Venkatramu, C.K. Jayasankar, Raman and photoluminescence studies of europium doped zinc-fluorophosphate glasses for photonic applications, J. Non Crystal. Solids 505 (2019) 115–121.

[51] M. Shoaib, G. Rooh, N. Chanthima, R. Rajaramakrishna, H.J. Kim, C. Wongdeeying, J. Kaewkhao, Intriguing energy transfer mechanism in oxide and oxy-fluoride phosphate glasses, Opt. Mater. 88 (2019) 429–444.

[52] P. Babu, C.K. Jayasankar, Optical spectroscopy of Eu3+ ions in lithium borate and lithium fluoroborate glasses, Physica B Condens. Matter 279 (2000) 262–281.

[53] M. Sołtys, J. Janek, L. Żur, J. Pisarska, W.A. Pisarski, Compositional-dependent europium-doped lead phosphate glasses and their spectroscopic properties, Opt. Mater. 40 (2015) 91–96.

[54] K. Anilkumar, D. S, S. Babu, V. Prasad, Y.C. Ratnakaram, 2018.

[55] V.R. Rao, L.L. Devi, C.K. Jayasankar, W. Pecharapa, J. Kaewkhao, S.R. Depuru, Luminescence and energy transfer studies of Ce3+/Dy3+ doped fluorophosphate glasses, J. Lumin. 208 (2019) 89–98.

[56] J. Pisarska, Optical properties of lead borate glasses containing Dy3+ions, J. Phys. Condens. Matter 21 (2009) 285101.

[57] S. Selvi, G. Venkataiah, S. Arunkumar, G. Muralidharan, K. Marimuthu, Structural and luminescence studies on Dy3+ doped lead boro–telluro-phosphate glasses, Phys. B Condens. Matter. 454 (2014) 72–81.

[58] E. Kaewnuam, N. Wantana, H.J. Kim, J. Kaewkhao, Development of lithium yttrium borate glass doped with Dy 3+ for laser medium, W-LEDs and scintillation materials applications, J. Non Cryst. Solids 464 (2017) 96–103.

[59] R. Praveena, R. Vijaya, C.K. Jayasankar, Photoluminescence and energy transfer studies of Dy3+-doped fluorophosphate glasses, Spectrochim. Acta Part A Mol. Biomol. Spectrosc. 70 (2008) 577–586.

[60] H. Ebendorff-Heidepriem, D. Ehrt, Effect of europium ions on X-ray-induced defect formation in phosphate containing glasses, Opt. Mater. 19 (2002) 351–363.

[61] D. Ehrt, P. Ebeling, U. Natura, UV Transmission and radiation-induced defects in phosphate and fluoride–phosphate glasses, J. Non Crystal. Solids 263–264 (2000) 240–250.

[62] H. Masai, G. Okada, A. Torimoto, T. Usui, N. Kawaguchi, T. Yanagida, X-ray-induced scintillation governed by energy transfer process in glasses, Sci. Rep. 8 (2018) 623.

[63] D.F. Jackson, D.J. Hawkes, X-ray attenuation coefficients of elements and mixtures, Phys. Rep. 70 (1981) 169–233.

[64] G. Yao, D. Valiev, S. Li, S. Stepanov, C. Li, H. Lin, L. Liu, Y. Zhou, F. Zeng, The luminescence performance of Tb3+ doped ABS-BGP glasses excited by different type of energy sources, J. Lumin. 226 (2020) 117514.